

# Sparse Channel Estimation for Multicarrier Underwater Acoustic Communication: From Subspace Methods to Compressed Sensing

Christian R. Berger\*, Shengli Zhou\*, James C. Preisig†, and Peter Willett\*

\*Dept. of Electrical and Computer Engr., University of Connecticut, Storrs, Connecticut 06269, USA

†Applied Ocean Physics and Engr. Dept., Woods Hole Oceanographic Institution, Woods Hole, MA 02543, USA

**Abstract**—In this paper, we present various channel estimators that exploit the channel sparsity in a multicarrier underwater acoustic system, including subspace algorithms from the array processing literature, namely root-MUSIC and ESPRIT, and recent compressed sensing algorithms in form of Orthogonal Matching Pursuit (OMP) and Basis Pursuit (BP). Numerical simulation and experimental data of an OFDM block-by-block receiver are used to evaluate the proposed algorithms in comparison to the conventional least-squares (LS) channel estimator. We observe that subspace methods can tolerate small to moderate Doppler effects, and outperform the LS approach when the channel is indeed sparse. On the other hand, compressed sensing algorithms uniformly outperform the LS and subspace methods. Coupled with a channel equalizer mitigating intercarrier interference, the compressed sensing algorithms can handle channels with significant Doppler spread.

**Index Terms**—OFDM, Doppler spread, ICI, MUSIC, ESPRIT, OMP, BP.

## I. INTRODUCTION

Underwater acoustic (UWA) channels have large delay spread and significant Doppler effects [1], and hence fall into the category of doubly (time- and frequency-) spread channels. One approach is to use a basis expansion model (BEM) to approximate the time-varying UWA channels, so that the number of unknowns in channel estimation can be reduced; see e.g., [2]–[4]. The other approach is to directly exploit the fact that UWA channels are naturally sparse, meaning that most channel energy is concentrated on a few delay and/or Doppler values [5], [6].

Sparse channel estimation has been extensively studied for frequency selective radio channels based on, e.g., subspace fitting [7], model order fitting using a generalized Akaike information criterion [8], zero-tap detection [9], or Monte Carlo Markov Chain methods [10]. More recently, advances in the new field of compressive sensing [11] have led to numerous applications on sparse channel estimation, e.g., [12]–[19]. Specifically on UWA channels, the matching pursuit (MP) algorithm and its variants have been used both in [5] for a single carrier system and in [20] for a multicarrier system.

As sparsity of the channel hinges on choosing an appropriate representation, we suggest to use a path-based representation. Specifically, we model the UWA channel based on a number of distinct paths, each characterized by a triplet of delay, Doppler rate, and path attenuation. When the channel has small Doppler spread, where the residual intercarrier interference (ICI) can be ignored after proper Doppler compensation, we show that subspace methods such as MUSIC and ESPRIT from the array processing literature [21] can be directly applied for sparse channel estimation. For channels with large Doppler spread, we adopt compressed sensing algorithms for sparse channel estimation, specifically in the form of Orthogonal Matching Pursuit (OMP) and Basis Pursuit (BP).

We use numerical simulation and experimental data to test the performance of the proposed sparse channel estimators, where the experimental data was recorded as part of the SPACE’08 experiment off the coast of Martha’s Vineyard, MA, from Oct. 14 to Nov. 1, 2008. We find that on channels with small to moderate Doppler effects, Root-MUSIC and ESPRIT channel estimators outperform the conventional least-squares (LS) scheme on sparse channels, but perform worse when most energy arrives as “diffuse” multipath. On the other hand, both OMP and BP can well handle sparse and diffuse multipath, performing uniformly the best, with BP having a slight edge over OMP. For channels with larger Doppler spread, BP and OMP algorithms continue to perform very well, as they can accommodate different Doppler scales on distinct paths. Drastic performance improvement is observed relative to the conventional LS method in channels with large Doppler spread.

The rest of this paper is as follows. In Section II we introduce the signal model. In Sections III and IV we present the subspace and compressed sensing algorithms, respectively. Sections V and VI contain simulation and experimental results, respectively. Conclusions are drawn in Section VII.

## II. SYSTEM MODEL

We consider zero-padded (ZP) orthogonal frequency division multiplexing (OFDM) as in [22]. Let  $T$  denote the OFDM symbol duration and  $T_g$  the guard interval for the ZP. The

C. R. Berger, S. Zhou, and P. Willett are supported by the ONR YIP grant N00014-07-1-0805, the ONR grant N00014-07-1-0429, and the NSF grants ECCS-0725562, CNS-0721834.

total OFDM block duration is  $T' = T + T_g$  and the subcarrier spacing is  $1/T$ . The  $k$ th subcarrier is at frequency

$$f_k = f_c + k/T, \quad k = -K/2, \dots, K/2 - 1, \quad (1)$$

where  $f_c$  is the carrier frequency and  $K$  subcarriers are used so that the bandwidth is  $B = K/T$ . Let  $s[k]$  denote the information symbol to be transmitted on the  $k$ th subcarrier. The non-overlapping sets of data subcarriers  $\mathcal{S}_D$ , pilot subcarriers  $\mathcal{S}_P$ , and null subcarriers  $\mathcal{S}_N$  satisfy  $\mathcal{S}_D \cup \mathcal{S}_P \cup \mathcal{S}_N = \{-K/2, \dots, K/2 - 1\}$ ; the null subcarriers are used to facilitate Doppler compensation at the receiver (see [22]).

The transmitted signal is given by

$$\tilde{x}(t) = \text{Re} \left\{ \left[ \sum_{k \in \mathcal{S}_D \cup \mathcal{S}_P} s[k] e^{j2\pi \frac{k}{T} t} q(t) \right] e^{j2\pi f_c t} \right\} \quad t \in [0, T + T_g], \quad (2)$$

where  $q(t)$  describes the zero-padding operation, i.e.,

$$q(t) = \begin{cases} 1 & t \in [0, T], \\ 0 & \text{otherwise.} \end{cases} \quad (3)$$

#### A. Channel Model

The underwater acoustic (UWA) time-varying channel model is often defined as

$$c(\tau, t) = \sum_p A_p(t) \delta(\tau - \tau_p(t)). \quad (4)$$

The time varying delays are caused by motion of the transmitter/receiver as well as scattering off of the moving sea surface or refraction due to sound speed variations. The path amplitudes change with the delays as the attenuation is related to the distance traveled as well as the physics of the scattering processes.

For the duration of an OFDM symbol, the time variation of the path delays can be reasonably approximated by a Doppler rate as,

$$\tau_p(t) = \tau_p - a_p t, \quad (5)$$

and the path amplitudes are assumed constant  $A_p(t) \approx A_p$ . Furthermore we assume that the UWA channel can be well approximated by  $N_p$  dominant discrete paths. With this, the channel model can be simplified to

$$c(\tau, t) = \sum_{p=1}^{N_p} A_p \delta(\tau - [\tau_p - a_p t]), \quad (6)$$

where we specifically keep the path dependent Doppler rates  $a_p$ . The received passband signal is then

$$\tilde{y}(t) = \sum_{p=1}^{N_p} A_p \tilde{x}([1 + a_p] t - \tau_p) + \tilde{n}(t), \quad (7)$$

where  $\tilde{n}(t)$  is additive noise.

#### B. Receiver Processing

A two-step approach to mitigating the channel Doppler effect was proposed in [22].

- 1) The first step is to resample  $\tilde{y}(t)$  in passband with a resampling factor  $\hat{a}$  that corresponds to a rough Doppler estimate, leading to  $\tilde{z}(t)$ , c.f. (9).
- 2) The second step is to perform fine Doppler shift compensation on  $\tilde{z}(t)$  to obtain  $\tilde{z}(t)e^{-j2\pi\epsilon t}$ , where  $\epsilon$  is the estimated residual mean Doppler shift.

The resampling can be written as the following:

$$\tilde{z}(t) = \sum_{p=1}^{N_p} A_p \tilde{x} \left( \left( \frac{1 + a_p}{1 + \hat{a}} \right) t - \tau_p \right) + \tilde{n}(t), \quad (8)$$

$$= \sum_{p=1}^{N_p} A_p \tilde{x} \left( (1 + b_p) (t - \tau'_p) \right) + \tilde{n}(t). \quad (9)$$

To simplify notation, we define the new residual Doppler rates and scaled delays

$$1 + b_p = 1 + \left( \frac{a_p - \hat{a}}{1 + \hat{a}} \right) = \frac{1 + a_p}{1 + \hat{a}}, \quad (10)$$

$$\tau'_p = \frac{\tau_p}{1 + b_p}. \quad (11)$$

Comparing (7) with (9), we see that the received waveform after resampling is equivalent to one that passed through a channel with Doppler rates  $b_p$ . In channels with a single dominant Doppler, e.g. from platform motion, this can reduce the channel to an ICI free system. In practice this operation will let us assume that the Doppler spread is centered around zero, as a non-zero mean of the  $a_p$  is removed by the resampling. The scaled delays only exchange the order of scaling and delaying.

Performing ZP-OFDM demodulation, the output  $z_m$  on the  $m$ th subchannel is

$$z_m = \frac{1}{T} \int_0^{T+T_g} z(t) e^{-j2\pi\epsilon t} e^{-j2\pi \frac{m}{T} t} dt, \quad (12)$$

where  $z(t)$  is the baseband version of  $\tilde{z}(t)$ . Plugging in  $z(t)$  and carrying out the integration, we simplify  $z_m$  to

$$z_m = \sum_{p=1}^{N_p} A_p e^{-j2\pi(f_m + \epsilon)\tau'_p} \sum_{k \in \mathcal{S}_D \cup \mathcal{S}_P} \varrho_{m,k}^{(p)} s[k] + v_m, \quad (13)$$

where  $v_m$  is the additive noise and

$$\varrho_{m,k}^{(p)} = \frac{\sin(\pi\beta_{m,k}^{(p)} T)}{\pi\beta_{m,k}^{(p)} T} e^{j\pi\beta_{m,k}^{(p)} T}, \quad (14)$$

$$\beta_{m,k}^{(p)} = (k - m) \frac{1}{T} + \frac{b_p f_m - \epsilon}{1 + b_p}. \quad (15)$$

Defining a stacked received vector  $\mathbf{z}$ , data vector  $\mathbf{s}$ , and noise vector  $\mathbf{v}$  across all subcarriers, we can write the following input-output relationship:

$$\mathbf{z} = \mathbf{H}\mathbf{s} + \mathbf{v}. \quad (16)$$

where the channel mixing-matrix  $\mathbf{H}$  has entries

$$[\mathbf{H}]_{m,k} = \sum_{p=1}^{N_p} A_p e^{-j2\pi(f_m + \epsilon)\tau'_p} \varrho_{m,k}^{(p)}. \quad (17)$$

The channel estimation methods in this paper use a base-band formulation where each path has a complex path gain. Specifically, the mixing matrix  $\mathbf{H}$  is now expressed as

$$\mathbf{H} = \sum_{p=1}^{N_p} \xi_p \mathbf{\Lambda}_p \mathbf{\Gamma}_p, \quad (18)$$

where the complex path gain for the  $p$ th path is

$$\xi_p = A_p e^{-j2\pi(f_c + \epsilon)\tau'_p}, \quad (19)$$

the matrix  $\mathbf{\Gamma}_p$  has an  $(m, k)$ th entry as  $[\mathbf{\Gamma}_p]_{m,k} = \varrho_{m,k}^{(p)}$ , and the matrix  $\mathbf{\Lambda}_p$  is a diagonal matrix with

$$[\mathbf{\Lambda}_p]_{m,m} = e^{-j2\pi \frac{m}{T} \tau'_p}. \quad (20)$$

The formulation in (18) clearly specifies the contribution from each discrete path with delay  $\tau'_p$  and Doppler scale  $b_p$  towards the channel mixing matrix.

### III. SUBSPACE METHODS

When all the paths have similar Doppler scales, proper choices of  $\hat{a}$  and  $\epsilon$  can render  $\mathbf{H}$  close to diagonal, which is the rationale for the receiver design in [22]. Specifically, the residual ICI is ignored, and  $\mathbf{\Gamma}_p$  in (18) is approximated by an identity matrix. Let us now relate this simplified setup to the direction finding problem from the array processing literature. Dividing the measurements,  $z_m$ , by the transmitted symbol on each subcarrier,  $s[m]$ , (in practice, only pilot subcarriers are considered, as will be clear later on), the estimated frequency responses can be collected into a vector, where we ignore the noise at this moment.

Collecting the diagonal entries of  $\mathbf{H}$  into a vector  $\tilde{\mathbf{h}}$ , we obtain

$$\tilde{\mathbf{h}} = \sum_{p=1}^{N_p} \xi_p \mathbf{w}(\tau'_p), \quad (21)$$

where  $\mathbf{w}(\tau'_p)$  has the  $m$ th entry  $e^{-j2\pi \frac{m}{T} \tau'_p}$ . The formulation in (21) is thus equivalent to a direction finding problem in the array processing literature; each arrival from a certain direction has a steering vector in a similar form to  $\mathbf{w}(\tau'_p)$ . Hence, subspace methods from array processing can be applied to identify the distinct path arrivals. Specifically, from the collected measurements, one needs to estimate the covariance matrix

$$\mathbf{R}_{\tilde{\mathbf{h}}} = E \left[ \tilde{\mathbf{h}} \tilde{\mathbf{h}}^H \right] = \sum_{p=1}^{N_p} E \left[ |\xi_p|^2 \right] \mathbf{w}(\tau'_p) \mathbf{w}(\tau'_p)^H. \quad (22)$$

The delays  $\{\tau'_p\}$ , corresponding to the directions in array processing, are identified based on eigen-decomposition of the covariance matrix  $\mathbf{R}_{\tilde{\mathbf{h}}}$ ,

Usually, a number of OFDM symbols (let's say  $I$ ) need to be observed to approximate the covariance matrix,  $\mathbf{R}_{\tilde{\mathbf{h}}} \approx$

$\frac{1}{I} \sum_{i=1}^I \tilde{\mathbf{h}}_i \tilde{\mathbf{h}}_i^H$ . In our work, we assume a block-by-block receiver as in [22]. Hence, we need to estimate the covariance matrix based on one OFDM symbol only. This is possible via spatial smoothing (see e.g. [23] or [21]). In a nutshell, as long as the steering vectors  $\mathbf{w}(\tau'_p)$  exhibit a shift invariance property, we can exchange the observations of a large array for multiple ‘‘independent’’ observations of a smaller array, but generated by the same  $\tau'_p$ .

Specifically, let us assume that the pilots are spaced uniformly within each OFDM symbol, i.e.,  $m = \Delta, 2\Delta, \dots$  and introduce a partial vector  $\tilde{\mathbf{h}}_a^b$ , which includes pilots  $a$  through  $b$  of the original vector. With that,

$$\tilde{\mathbf{h}}_{a+\delta}^{b+\delta} = \sum_{p=1}^{N_p} \xi_p \mathbf{w}_{a+\delta}^{b+\delta}(\tau'_p) \quad (23)$$

$$= \sum_{p=1}^{N_p} \left( \xi_p e^{-j2\pi \delta \frac{a}{T} \tau'_p} \right) \mathbf{w}_a^b(\tau'_p) \quad (24)$$

which can be interpreted as a second observation of  $\tilde{\mathbf{h}}_a^b$  with new amplitudes  $\xi_p e^{-j2\pi \delta \frac{a}{T} \tau'_p}$ . We therefore approximate the covariance matrix of size  $N_C = b - a$  as,

$$\mathbf{R}_{\tilde{\mathbf{h}}}^{N_C} \approx \frac{1}{I} \sum_{i=1}^I \tilde{\mathbf{h}}_i^{i+N_C} \left( \tilde{\mathbf{h}}_i^{i+N_C} \right)^H \quad (25)$$

where  $I = K/\Delta - N_C + 1$  depends on the number of available observations (pilots). Clearly there is a trade off: a larger  $N_C$  leads to better resolution of the  $\tau'_p$ , while a larger  $I$  approximates the covariance matrix better. In any case both dimensions have to be larger than the assumed maximum number of paths, as the rank of the covariance matrix limits the maximum number of identifiable components.

#### A. Root-MUSIC

We choose the unitary implementation of Root-MUSIC, to reduce computational complexity (for details see [21]). The order selection problem is solved in the following way: after matrix decomposition of the covariance matrix, we choose all eigenvectors corresponding to eigenvalues less than twice the noise variance to compose the noise space.

Once the  $\{\tau'_p\}$  are estimated, the channel response on the data subcarriers are estimated by using the LS solution to (21) based on the channel frequency responses on the pilot subcarriers.

#### B. ESPRIT

As for Root-MUSIC, we choose the unitary implementation for ESPRIT, following the details in [24] or [21]. The signal space is determined complementary to the noise subspace in MUSIC; we choose all eigenvectors corresponding to eigenvalues larger or equal to twice the noise variance. To improve robustness against model mismatch (especially caused by Doppler), we solve for the unknown delay parameters  $\tau'_p$  using a total-least-squares (TLS) formulation. Then the channel response on the data subcarriers is determined as in Sec. III-A.

#### IV. COMPRESSED SENSING

Although  $\mathbf{H}$  has  $K^2$  entries, it is defined by  $N_p$  triples of  $(\xi_p, b_p, \tau'_p)$ . Since UWA channels are sparse, the value of  $N_p$  is small, hence, it is possible that those  $N_p$  paths can be identified by compressed sensing methods based on only a limited number of measurements.

To facilitate implementation, we rewrite  $\mathbf{z}$  as

$$\mathbf{z} = [\mathbf{\Lambda}_1 \mathbf{\Gamma}_1 \mathbf{s} \quad \cdots \quad \mathbf{\Lambda}_{N_p} \mathbf{\Gamma}_{N_p} \mathbf{s}] \begin{bmatrix} \xi_1 \\ \vdots \\ \xi_{N_p} \end{bmatrix} + \mathbf{v}. \quad (26)$$

If the parameters  $(b_p, \tau'_p)$  were available, we could construct the  $(K \times N_p)$ -matrix in (26) and solve for the  $\xi_p$  using the least-squares solution.

##### A. Non-Linear Estimation via Compressed Sensing

A brute force approach to solve (26) would be to try all possible combinations of  $\{(b_p, \tau'_p)\}_{p=1}^{N_p}$  and choose the solution with the best fit. Of course the fit always improves as a function of  $N_p$ , which is unknown. Similar estimation problems have been solved using compressed sensing [11], where a problem, given as a linear combination of an unknown number of signals defined by an equivalent number of parameters (sets), is solved by constructing a so-called dictionary, made of the signals parameterized by a representative selection of possible parameter sets. In this model, parameter sets not part of the solution will be assigned a zero weight coefficient. Since a large number of such sets is necessary to construct an accurate dictionary, most weights will be zero and the problem is sparse.

We follow this approach and choose representative sets of  $(b, \tau')$  as,

$$\tau' \in \left\{ 0, \frac{T}{\lambda K}, \frac{2T}{\lambda K}, \dots, T_g \right\}, \quad (27)$$

$$b \in \{-b_{\max}, -b_{\max} + \Delta b, \dots, b_{\max}\}. \quad (28)$$

The discretization in  $\tau'$  is based on the assumption that after synchronization all arriving paths fall into the guard interval, where we choose the time resolution as a multiple,  $\lambda$ , of the baseband sampling time  $T/K$ , leading to  $N_\tau = \lambda K T_g / T$  tentative delays. For the residual Doppler rates, we assume that they are spread around zero after compensation by  $\hat{a}$ , and  $b_{\max}$  can be chosen based on the assumed Doppler spread, with resolution  $2b_{\max}/(\Delta b) + 1 = N_b$ . Hence, a total of  $N_\tau N_b$  candidate paths will be searched, and we expect  $N_p \ll N_\tau N_b$  significant paths due to the channel sparsity.

With this, we form vectors  $\mathbf{x}_A^{(i)} = [\xi_1^{(i)}, \dots, \xi_{N_\tau}^{(i)}]^T$ , corresponding to all delays associated with Doppler scale  $b_i$ , and form a vector  $\mathbf{x} = [(\mathbf{x}_A^{(1)})^T, \dots, (\mathbf{x}_A^{(N_b)})^T]^T$ . The linear formulation of the problem is that

$$\begin{aligned} \mathbf{z} &= [\mathbf{\Lambda}_1 \mathbf{\Gamma}_1 \mathbf{s} \quad \cdots \quad \mathbf{\Lambda}_{N_\tau N_b} \mathbf{\Gamma}_{N_\tau N_b} \mathbf{s}] \mathbf{x} + \mathbf{v} \\ &:= \mathbf{A} \mathbf{x} + \mathbf{v} \end{aligned} \quad (29)$$

where  $\mathbf{A}$  is a fat matrix with  $N_\tau N_b$  columns, and most of entries of  $\mathbf{x}$  are assumed to be zeros due to channel sparsity.

#### B. BP and OMP Algorithms

To solve the sparse estimation problem with the measurement model in (29), there are two popular algorithms (and variants of them):

- 1) Basis Pursuit, for an efficient implementation see [25].
- 2) (Orthogonal) Matching Pursuit, see e.g., [5].

Due to the lack of space, we skip the implementation details. For implementations of these algorithms, it is important to consider that multiplying by the matrix  $\mathbf{A}$  can be done efficiently using FFTs.

To reduce the complexity of computing the dictionary set with a large size, we choose to retain only  $D$  off diagonals on the templates  $\mathbf{\Gamma}_p$ , (therefore also on  $\mathbf{H}$ ). This means that only ICI from  $D$  directly neighboring subcarriers on each side are considered. The symbol vector  $\mathbf{s}$  contains known pilot symbols, and zeros, but also unknown data symbols. The unknown data symbols are set to zero to compute the matrix  $\mathbf{A}$ .

Once the channel mixing matrix is constructed, a zero-forcing receiver is applied for data demodulation followed by channel decoding for data recovery. The special case of  $D = 0$  corresponds to an ICI-ignorant receiver.

#### V. SIMULATION RESULTS

In simulation, we approximate the continuous time operations in (12) with a sampling rate being twice the bandwidth. The channel model uses  $N_p = 15$  discrete paths, with the inter-arrival times distributed exponentially with mean  $E[\tau_{p+1} - \tau_p] = 1$  ms. Hence, the average channel delay spread is about 15 ms. The amplitudes are Rayleigh distributed with the average power decreasing exponentially with delay, where the difference between the beginning and the end of the guard time of 24.6 ms is 20 dB. Each path has a Doppler rate drawn from a zero mean uniform distribution. With the velocity standard deviation  $\sigma_v$ , the maximum possible Doppler is  $\sqrt{3}\sigma_v f_c / c$  (the sound speed is set to  $c = 1500$  ms). We choose a zero-mean Doppler distribution, because a non-zero mean could be removed through the resampling operation.

The carrier frequency is set to  $f_c = 13$  kHz and the bandwidth is  $B = 9.77$  kHz. The total number of subcarriers is  $K = 1024$ , which leads to a subcarrier spacing of  $\Delta f = 9.54$  Hz and a symbol interval of  $T = 104.86$  ms. A guard time of  $T_g = 24.6$  ms is inserted between consecutive OFDM blocks.

##### A. ICI-Ignorant Receiver

We first compare the performance of different receivers assuming that the residual ICI after proper Doppler compensation can be ignored, as in [22], [26], [27]. We adopt the subcarrier allocation from [27]. Out of the  $K = 1024$  subcarriers, there are  $|\mathcal{S}_P| = 256$  subcarriers carrying pilot symbols, distributed on every fourth subcarrier, and  $|\mathcal{S}_N| = 96$  zeros, half at the band edges and half inserted randomly between the data. The remaining 672 data subcarriers are encoded using a rate 1/2 nonbinary LDPC code (see [27] for

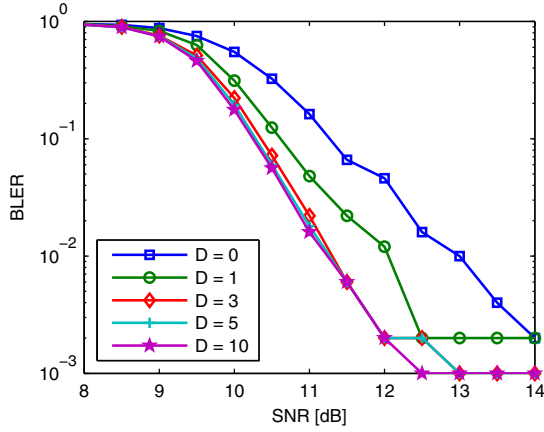


Fig. 1. Perfect channel knowledge, but only  $D$  off-diagonals from each side are kept in the channel matrix for data demodulation. The channel has a mild Doppler spread with  $\sigma_v = 0.1$  m/s.

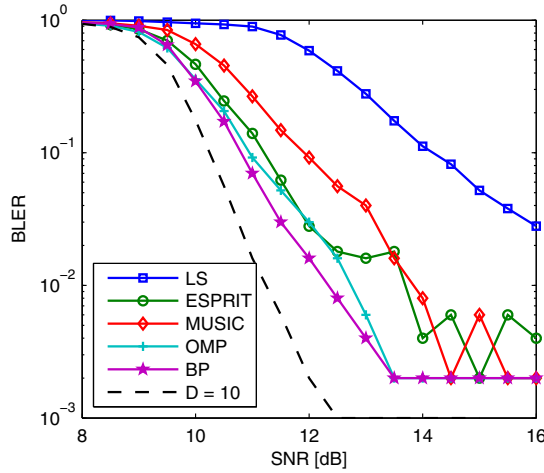


Fig. 2. Performance comparisons for ICI-ignorant receivers with different channel estimation methods.

details). With a 16-QAM constellation, the spectral efficiency  $\alpha$  and the data rate  $R$  are

$$\alpha = \frac{T}{T + T_g} \cdot \frac{672}{1024} \cdot \frac{1}{2} \cdot \log_2 16 = 1.1 \text{ bits/s/Hz}, \quad (30)$$

$$R = \alpha B = 10.4 \text{ kb/s}. \quad (31)$$

Each simulation uses 500 OFDM symbols.

*Test Case 1):* We first assume that the receiver has perfect knowledge of all path amplitudes, delays, and Doppler rates. However, the channel mixing matrix  $\mathbf{H}$  in (16) will be approximated with a banded structure keeping  $D$  off-diagonals to each side (i.e., a total of  $2D+1$  diagonals are retained). Fig. 1 shows the block error rate (BLER) performance for different  $D$ , where the channel has mild Doppler spread with  $\sigma_v = 0.1$  m/s. We observe that the ICI ignorant receiver ( $D = 0$ ) works well, being about 2 dB away from the full matrix case. Most of the ICI can be captured by a banded matrix approximation with  $D = 3$ .

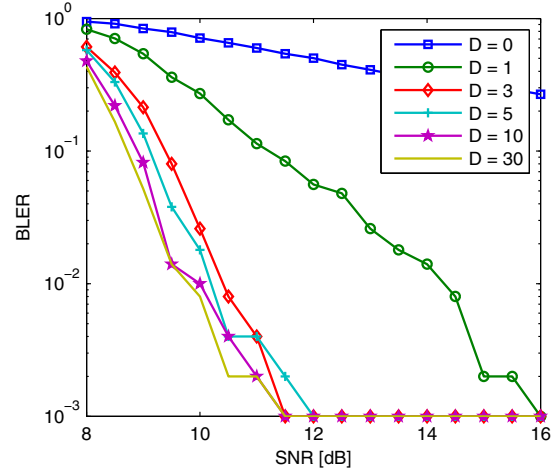


Fig. 3. Perfect channel knowledge, but only  $D$  off-diagonals from each side are kept in the channel matrix for data demodulation. The channel has a severe Doppler spread with  $\sigma_v = 0.25$  m/s.

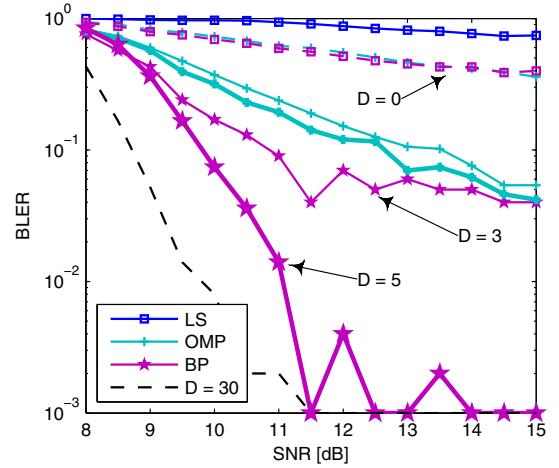


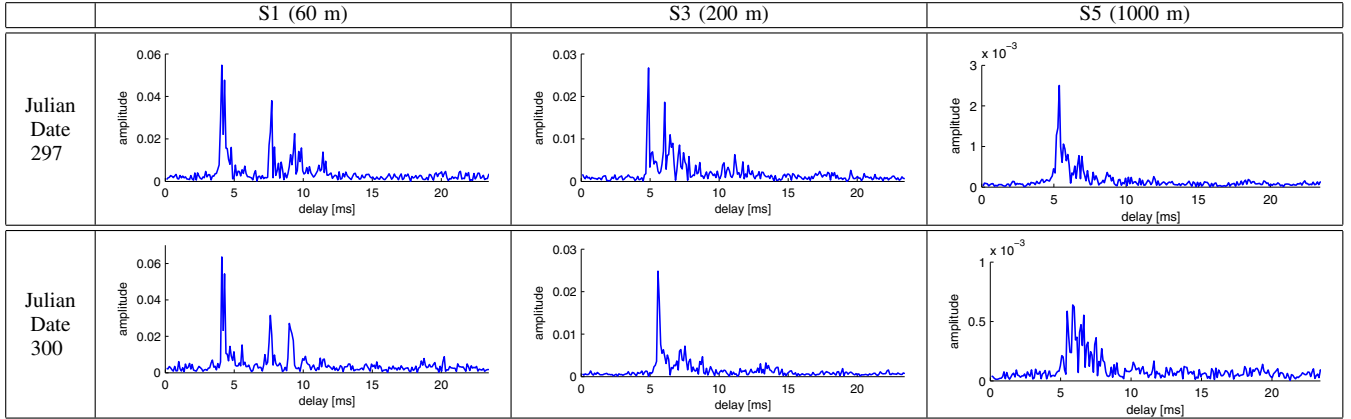
Fig. 4. Performance comparisons for ICI aware receivers, where the channel mixing matrix is assumed to have  $D$  off diagonals from each side.

*Test Case 2):* In Fig. 2, we compare the ICI-ignorant receivers ( $D = 0$ ) with channels estimated from the five considered methods. We find that all receivers achieve a low BLER, but at different levels of SNR. Clearly all sparse channel estimation schemes outperform the simple least-squares (LS) channel estimator (see [22] for details), gaining about 2 dB. Between the sparse channel estimators, the compressed sensing based algorithms outperform the subspace algorithms slightly. Another drawback of the subspace based algorithms is that they occasionally seem to fail, noticeable by a fluctuating error floor.

### B. ICI-Aware Receiver

We now consider channels with more severe Doppler spreads. To improve the channel estimation performance in the presence of severe ICI, we convert 96 data subcarriers into additional pilots by assuming that 96 data symbols are known a priori. The additional pilots are grouped in clusters

TABLE I  
EXAMPLES OF CHANNEL RESPONSES FROM THE SPACE'08 EXPERIMENT, TAKEN FROM THE LS ESTIMATE.



between zero subcarriers and existing pilots, creating groups of five consecutive known subcarriers. Adjacent observations are needed as to effectively estimate the Doppler rate  $b_p$  of each path by observing the ICI.

Since 96 coded symbols are assumed known while the same LDPC code structure is used, this leads to an equivalent coding rate of  $(336 - 96)/(672 - 96) \approx 0.4$ . With 16-QAM constellation, the spectral efficiency and the data rate are

$$\alpha = \frac{T}{T + T_g} \cdot \frac{336 - 96}{1024} \cdot \log_2 16 = 0.76 \text{ bits/s/Hz}, \quad (32)$$

$$R = \alpha B = 7.4 \text{ kb/s}. \quad (33)$$

*Test Case 3):* We first assume that the channel is known. The numerical simulation results are depicted in Fig. 3. where  $\sigma_v = 0.25$  m/s. Clearly ICI-ignorant receivers ( $D = 0$ ) have very poor performance, which indicates the need for ICI-aware receivers. We also notice that in the full CSI case, once we remove sufficient levels of ICI the performance is about 1 dB better than in Fig. 1(a), due to the change in coding rate.

*Test Case 4):* The channel with significant Doppler spread can only be handled by the compressed sensing based estimators. In addition to delay, we introduce dictionaries that also consider fifteen different Doppler rates uniformly distributed within  $[-b_{\max}, b_{\max}]$ , where  $b_{\max} = v_{\max}/c = 5 \cdot 10^{-4}$ . As comparison we include the LS and the OMP/BP algorithms that assume no Doppler as previously ( $D = 0$ ), but benefit from the increased number of pilots. Simulation results are in Fig. 4. We observe that performance significantly improves by considering ICI explicitly through the increase of  $D$ . For channels with large Doppler spread, we notice that the improvement of BP over OMP increases.

## VI. EXPERIMENTAL RESULTS

The experimental data was recorded as part of the SPACE'08 experiment off the coast of Martha's Vineyard, MA, from Oct. 14 to Nov. 1, 2008. The water depth was about 15 meters. We consider three receivers, labeled as S1, S3, and S5, which were 60 m, 200 m, and 1,000 m from

the transmitter, respectively. Each receiver array has at least twelve hydrophones. We plot the performance combining an increasing number of phones to increase the effective SNR and show performance differences. We always combine the phones starting from phone one, then one and two, and so on. We consider recorded data from two different days, Julian Dates 297 and 300, where one day has rather calm sea and one day has more wind activity, respectively. There are between one hundred and two hundred of OFDM symbols per day, used to generate the performance plots.

### A. ICI-Ignorant receivers

The OFDM parameters are identical to those in Sec. V-A; hence, the achieved spectral efficiency and the data rate are in (30) and (31), respectively.

In this subsection, we test ICI-ignorant receivers. The sample channel responses based on the LS estimators at different receiver locations are shown in Table I.

1) *S1 Data (60 m):* At a short distance of only 60 m and considering the shallow water depth, we expect rich multipath and significant Doppler variation due to the geometry. This makes this receiver the most challenging in terms of channel response, but the easiest in terms of received signal strength or SNR. From Table I, we notice that there are three to four significant clusters of similar strength.

In Fig. 5 we see the BLER performance for Julian Dates 297 and 300. As in the numerical simulation the order of compressed sensing, subspace, LS stays the same, although MUSIC and ESPRIT switch places, and LS outperforms the subspace methods initially. In general this setup is challenging and we notice error floors.

2) *S3 Data (200 m):* The middle distance might be the best tradeoff between channel difficulty and received SNR. The example channel responses in Table I seem to be more contained, with a more dominating first cluster. The BLER performance in Fig. 5 is much better compared to the S1 receiver, where in the calm day (Julian Date 297) LS surprisingly outperforms the subspace methods. This could be connected

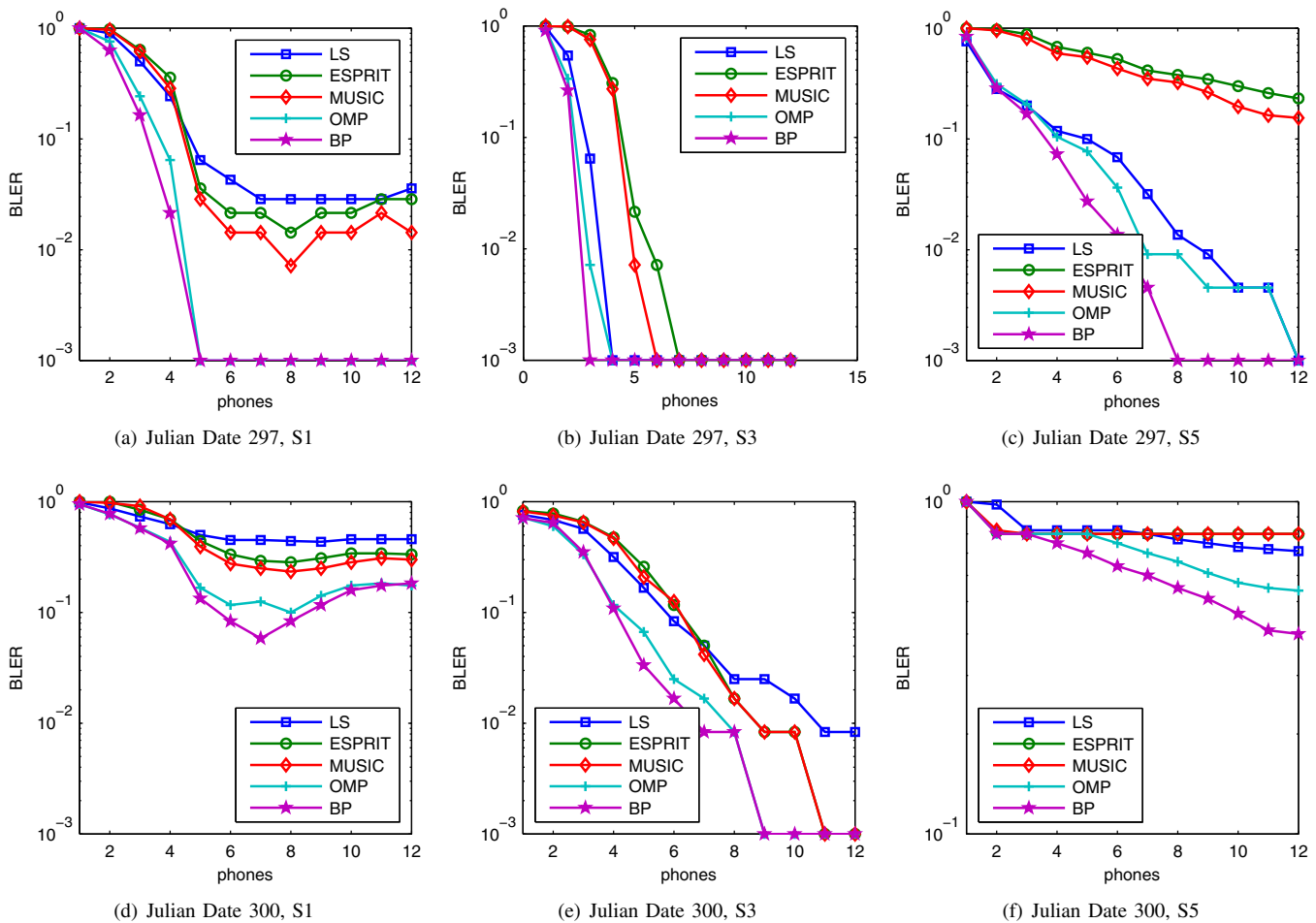


Fig. 5. Performance results using ICI-ignorant receivers at three different locations (S1, S3, and S5) on two Julian dates.

to the subspace methods assuming discrete tones and being more keyed towards detecting them instead of recreating the effect of possibly diffuse components.

3) *S5 Data (1000 m)*: At the 1 km distance only one significant cluster can be spotted in the channel estimates, and at the stormy day (Julian Date 300) the received energy seems to be vanishingly small, c.f. Table I. Accordingly the trend of the LS channel estimator closing in on the compressed sensing algorithms continues, with the subspace methods not able to handle this diffuse multipath. On the stormy day the performance is generally bad, with the best being BP successfully recovering little more than half of the OFDM blocks.

### B. ICI-Aware Receivers

We saw that on the stormy day (Julian Date 300), the performance was limited, most likely due to ICI caused by significant Doppler spread that cannot be handled by the ICI-ignorant receivers. We now focus on Julian Date 300 to test the effectiveness of ICI-aware receivers based on compressed sensing.

The OFDM parameters are identical to those in Section V-B; hence, the achieved spectral efficiency and the data rate are in (30) and (31), respectively.

As shown in Fig. 6, the performance improvement of the ICI-aware receivers ( $D = 3$ ) relative to ICI-ignorant receivers ( $D = 0$ ) is evident. Comparing Fig. 6 with Fig. 5, we also notice that the LS algorithm benefits from the additional pilots and coding, but its performance is much worse than the BP/OMP alternatives.

## VII. CONCLUSION

We considered sparse channel estimation using subspace methods and compressed sensing on channels with small to moderate Doppler effects, and extended the compressed sensing receivers to handle channels with different Doppler scales on different paths. In comparison to the LS receiver we found that the subspace methods show significant performance increase on channels that are sparse, but perform worse if most received energy comes from diffuse multipath. Compressed sensing algorithms, namely OMP and BP, do not suffer this drawback. When accounting for different Doppler scales on different paths, BP and OMP can handle channels in very

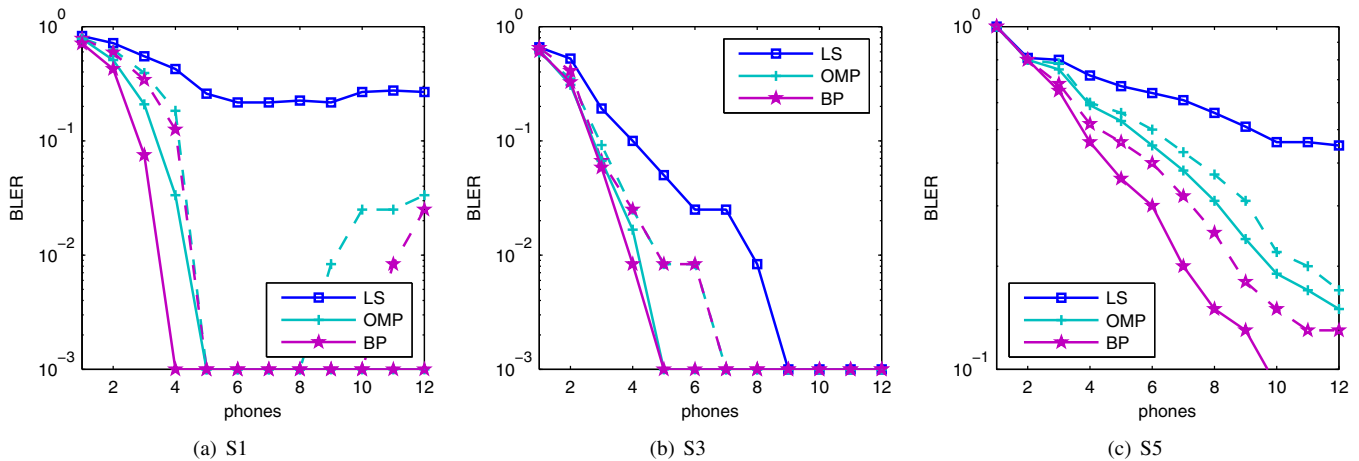


Fig. 6. Performance results using the ICI-aware receivers, Julian date 300, (dashed lines  $D = 0$ , solid lines  $D = 3$ ).

challenging conditions.

#### REFERENCES

- [1] T. H. Eggen, A. B. Baggeroer, and J. C. Preisig, "Communication over Doppler spread channels. Part I: Channel and receiver presentation," *IEEE J. Ocean. Eng.*, vol. 25, no. 1, pp. 62–71, Jan. 2000.
- [2] F. Qu and L. Yang, "Basis expansion model for underwater acoustic channels?" in *Proc. of MTS/IEEE OCEANS Conf.*, Québec City, Québec, Sep. 2008.
- [3] S.-J. Hwang and P. Schniter, "Efficient multicarrier communication for highly spread underwater acoustic channels," *IEEE J. Select. Areas Commun.*, vol. 26, no. 9, pp. 1674–1683, Dec. 2008.
- [4] G. Leus and P. A. van Walree, "Multiband OFDM for covert acoustic communications," *IEEE J. Select. Areas Commun.*, vol. 26, no. 9, pp. 1662–1673, Dec. 2008.
- [5] W. Li and J. C. Preisig, "Estimation of rapidly time-varying sparse channels," *IEEE J. Ocean. Eng.*, vol. 32, no. 4, pp. 927–939, Oct. 2007.
- [6] M. Stojanovic, "OFDM for underwater acoustic communications: Adaptive synchronization and sparse channel estimation," in *Proc. of Intl. Conf. on Acoustics, Speech and Signal Proc.*, Las Vegas, NV, Apr. 2008.
- [7] C.-J. Wu and D. W. Lin, "Sparse channel estimation for OFDM transmission based on representative subspace fitting," in *Proc. of Vehicular Technology Conference*, Stockholm, Sweden, May 2005.
- [8] M. R. Raghavendra and K. Giridhar, "Improving channel estimation in OFDM systems for sparse multipath channels," *IEEE Signal Processing Lett.*, vol. 12, no. 1, pp. 52–55, Jan. 2005.
- [9] C. Carbonelli, S. Vedantam, and U. Mitra, "Sparse channel estimation with zero tap detection," *IEEE Trans. Wireless Commun.*, vol. 6, no. 5, pp. 1743–1763, May 2007.
- [10] O. Rabaste and T. Chonavel, "Estimation of multipath channels with long impulse response at low SNR via an MCMC method," *IEEE Trans. Signal Processing*, vol. 55, no. 4, pp. 1312–1325, Apr. 2007.
- [11] R. Baraniuk, "Compressive sensing," *IEEE Signal Processing Magazine*, vol. 24, no. 4, pp. 118–121, Jul. 2007.
- [12] S. F. Cotter and B. D. Rao, "Sparse channel estimation via matching pursuit with application to equalization," *IEEE Trans. Commun.*, vol. 50, no. 3, pp. 374–377, Mar. 2002.
- [13] G. Z. Karabulut and A. Yongacoglu, "Sparse channel estimation using orthogonal matching pursuit algorithm," in *Proc. of Vehicular Technology Conference*, Los Angeles, CA, Sep. 2004.
- [14] C. Carbonelli and U. Mitra, "A simple sparse channel estimator for underwater acoustic channels," in *Proc. of MTS/IEEE OCEANS Conf.*, Vancouver, Canada, Oct. 2007.
- [15] C.-J. Wu and D. W. Lin, "A group matching pursuit algorithm for sparse channel estimation for OFDM transmission," in *Proc. of Intl. Conf. on Acoustics, Speech and Signal Proc.*, Toulouse, France, May 2006.
- [16] N. Richard and U. Mitra, "Sparse channel estimation for cooperative underwater communications: A structured multichannel approach," in *Proc. of Intl. Conf. on Acoustics, Speech and Signal Proc.*, Las Vegas, NV, Apr. 2008.
- [17] B. Friedlander, "Random projections for sparse channel estimation and equalization," in *Proc. of Asilomar Conf. on Signals, Systems, and Computers*, Pacific Grove, CA, Oct. 2006.
- [18] W. U. Bajwa, J. Haupt, G. Raz, and R. Nowak, "Compressed channel sensing," in *Proc. of Conf. on Information Sciences and Systems (CISS)*, Princeton, NJ, Mar. 2008.
- [19] M. Sharp and A. Scaglione, "Application of sparse signal recovery to pilot-assisted channel estimation," in *Proc. of Intl. Conf. on Acoustics, Speech and Signal Proc.*, Las Vegas, NV, Apr. 2008.
- [20] T. Kang and R. A. Iltis, "Iterative carrier frequency offset and channel estimation for underwater acoustic OFDM systems," *IEEE J. Select. Areas Commun.*, vol. 26, no. 9, pp. 1650–1661, Dec. 2008.
- [21] H. Van Trees, *Optimum Array Processing*, 1st ed., ser. Detection, Estimation, and Modulation Theory (Part IV). New York: John Wiley & Sons, Inc., 2002.
- [22] B. Li, S. Zhou, M. Stojanovic, L. Freitag, and P. Willett, "Multicarrier communication over underwater acoustic channels with nonuniform Doppler shifts," *IEEE J. Ocean. Eng.*, vol. 33, no. 2, Apr. 2008.
- [23] T.-J. Shan, M. Wax, and T. Kailath, "On spatial smoothing for direction-of-arrival estimation of coherent signals," *IEEE Trans. Signal Processing*, vol. 33, no. 4, pp. 806–811, Aug. 1985.
- [24] M. Pesavento, A. B. Gershman, and M. Haardt, "Unitary root-MUSIC with a real-valued eigendecomposition: A theoretical and experimental performance study," *IEEE Trans. Signal Processing*, vol. 48, no. 5, pp. 1306–1314, May 2000.
- [25] S.-J. Kim, K. Koh, M. Lustig, S. Boyd, and D. Gorinevsky, "An interior-point method for large-scale  $l_1$ -regularized least squares," *IEEE J. Select. Topics Signal Proc.*, vol. 1, no. 4, pp. 606–617.
- [26] S. Mason, C. R. Berger, S. Zhou, and P. Willett, "Detection, synchronization, and doppler scale estimation with multicarrier waveforms in underwater acoustic communication," *IEEE J. Select. Areas Commun.*, vol. 26, no. 9, Dec. 2008.
- [27] J. Huang, S. Zhou, and P. Willett, "Nonbinary LDPC coding for multicarrier underwater acoustic communication," *IEEE J. Select. Areas Commun.*, vol. 26, no. 9, pp. 1684–1696, Dec. 2008.